CHILEAN JOURNAL of AGRICULTURAL RESEARCH
RESEARCH ARTICLE

Green synthesis and biological activity of silver nanoparticles mediated by *Hypericum perforatum* L. and the endemic *H. malatyanum* Peşmen

Elif Özbey[1*]

[1]Malatya Turgut Özal University, Battalgazi Vocational School, Department of Park and Horticultural Crops Malatya, Türkiye.
[*]Corresponding author (elif.ozbey@ozal.edu.tr)
Received: 26 March 2026; Accepted: 15 July 2026, Available online: 7 September 2026. doi:10.4067/S0718-58392026000600898

ABSTRACT

Plant-mediated green synthesis of nanoparticles has gained increasing attention as an environmentally friendly alternative to conventional chemical synthesis. In this study, the phytochemical properties and antioxidant capacities of *Hypericum perforatum* L. and the endemic *H. malatyanum* Peşmen were determined, and their potential for the biosynthesis of Ag nanoparticles (AgNPs) was comparatively evaluated. *Hypericum malatyanum* exhibited higher total phenolic content (231.4 ± 5.8 *vs*. 216.9 ± 4.4 mg GAE g^{-1}), DPPH radical scavenging activity (79.9 ± 0.9% *vs*. 73.8 ± 1.6%), and FRAP values (315.5 ± 8.6 *vs*. 269.6 ± 7.7 µmol Fe^{2+} g^{-1}) than *H. perforatum*, whereas *H. perforatum* contained higher total flavonoid content and ABTS radical scavenging activity. The biosynthesized AgNPs were characterized by Fourier transform infrared spectroscopy, X-ray diffraction, scanning electron microscopy (SEM), and energy dispersive X-ray spectroscopy analyses. The SEM images revealed predominantly spherical nanoparticles with sizes ranging from 1 to 80 nm. Antimicrobial activity was evaluated using disk diffusion and minimum inhibitory concentration (MIC) assays. The AgNPs synthesized using *H. malatyanum* generally exhibited stronger antimicrobial activity and lower MIC values than those synthesized using *H. perforatum*. The highest antimicrobial activity was observed against *Bacillus spizizenii*, with an inhibition zone of 7.45 ± 0.087 mm and a MIC value of 6.25 mg mL^{-1}. The lowest MIC value (6.25 mg mL^{-1}) was also recorded against *Streptococcus pyogenes*, *Enterococcus faecalis*, and *Klebsiella pneumoniae* for *H. malatyanum*-derived AgNPs. These findings demonstrate that differences in phytochemical composition among *Hypericum* species influence AgNP formation and biological performance and highlight endemic species as promising biological resources for the sustainable production of antimicrobial nanomaterials.

Key words: Antimicrobial activity, green synthesis, *Hypericum malatyanum*, *Hypericum perforatum*, phytochemicals, silver nanoparticles.

INTRODUCTION

The genus *Hypericum* belongs to the family Clusiaceae (Guttiferae, Hypericaceae) and comprises approximately 500 species distributed worldwide, except Antarctica (Crockett and Robson, 2011). In Türkiye, the genus is represented by nearly 100 taxa, of which 47 are endemic (Güner et al., 2012). Among these, *H. perforatum* L. is the most widely recognized and extensively used species due to its medicinal properties, while *H. malatyanum* Peşmen is an endemic species with a highly restricted distribution in the rocky habitats of Malatya province (Figure 1) (Peşmen, 1980). The ecological adaptation and limited distribution of endemic species often lead to distinct biochemical profiles, which may contribute to their biological and functional potential.

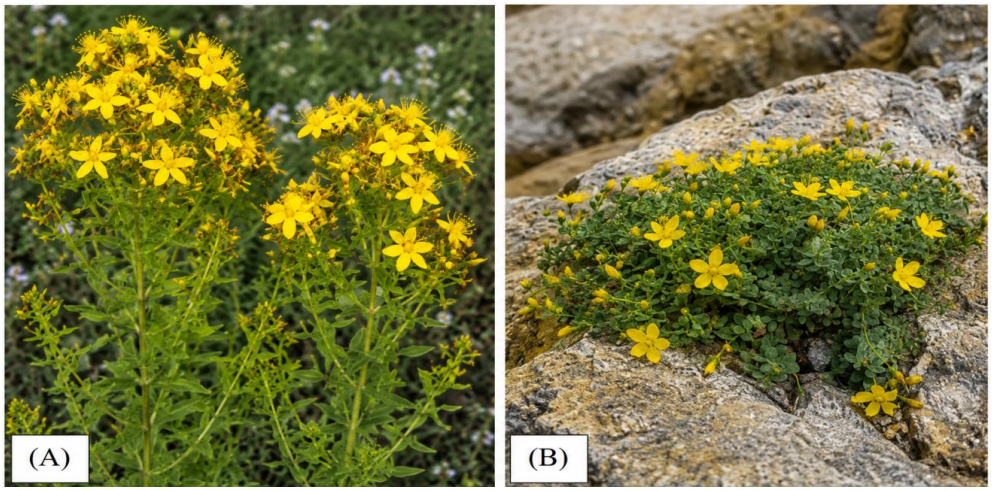

Figure 1. Morphological appearance of *Hypericum* species used in the study: *Hypericum perforatum* L. (Popay, 2015) (A); *Hypericum malatyanum* Peşmen (Dirmenci and Robson, 2019) (B)

Species of *Hypericum* are known to be rich in bioactive compounds such as anthraquinones (e.g., hypericin), prenylated phloroglucinols (e.g., hyperforin), flavonoids, biflavonoids, and phenolic acids. These phytochemicals are strongly associated with antioxidant and antimicrobial properties and play a crucial role in plant defense mechanisms (Özbey et al., 2025). In recent years, increasing attention has been directed toward the evaluation of total phenolic and flavonoid contents, along with antioxidant capacity, as indicators of plant bioactivity and functional value (Çırak and Kurt, 2014). Such phytochemical richness not only contributes to traditional medicinal uses but also provides a promising biochemical foundation for emerging biotechnological applications.

With the rapid advancement of nanotechnology, environmentally friendly approaches for nanoparticle synthesis have gained importance. Conventional physical and chemical methods often involve toxic reagents and high energy requirements, whereas biological synthesis offers a sustainable alternative (Patil and Kim, 2018; Saravanakumar et al., 2018). Plant extracts, in particular, have been widely employed in the green synthesis of Ag nanoparticles (AgNPs), as their phytochemical constituents, especially phenolics and flavonoids, act as both reducing and stabilizing agents (Srikar et al., 2016). Similar plant-mediated synthesis studies have also demonstrated the antimicrobial potential of biosynthesized AgNPs (Baran, 2019). Moreover, antioxidant-rich plant matrices can enhance nanoparticle formation efficiency and influence their biological activity. Recent studies have further demonstrated that plant-derived nanoparticles can improve plant stress tolerance and exhibit multiple biological functions, highlighting their broad agricultural and biotechnological potential (Alowaiesh et al., 2024). Beyond their synthesis, nanoparticles are increasingly applied in plant systems for improving growth performance, protection, and targeted delivery of bioactive compounds (Çiftçi and Altınkut-Uncuoğlu, 2019).

Silver nanoparticles have attracted considerable interest due to their antimicrobial potential and diverse applications in medicine, agriculture, food technology, and environmental systems (Satpathy et al., 2018). Recent studies highlight that phytochemical-driven synthesis may improve nanoparticle stability and bioactivity compared to chemically synthesized counterparts (Ojo et al., 2017).

Despite the increasing number of studies on plant-mediated synthesis of AgNPs, comparative studies evaluating the influence of phytochemical composition of closely related plant species on nanoparticle formation and biological activity remain limited. In particular, endemic plant species may possess unique phytochemical profiles that could significantly affect nanoparticle synthesis efficiency and functional properties. Therefore, the aim of this study was to investigate the phytochemical characteristics and antioxidant capacities of *H. perforatum* and the endemic species *H. malatyanum* and to evaluate their potential for the green synthesis of AgNPs. In addition, the antimicrobial activities of the synthesized nanoparticles were comparatively assessed against selected bacterial and yeast strains. We hypothesized that phytochemical differences between endemic and widely distributed species influence nanoparticle synthesis efficiency and antimicrobial activity.

MATERIALS AND METHODS

Plant material

Hypericum perforatum L. was collected from the Medicinal and Aromatic Plants Garden at Malatya Turgut Özal University Battalgazi Vocational School. The endemic species *H. malatyanum* Peşmen was collected from rocky slopes at an altitude of 1680 m in Meletbaşı (Eskiköy, Doğanşehir, Malatya, Türkiye) during the first week of July. The above-ground parts of the plants were dried at room temperature for 1 wk. The dried materials were ground to pass through a 1 mm sieve and stored in dark conditions until analysis.

Extraction and phytochemical analyses total phenolic and flavonoid content

Powdered plant material (10 g) was extracted with 100 mL methanol in a water bath at 60 °C for 24 h. The extracts were filtered through Whatman filter paper and stored at 4 °C until further analyses.

Total phenolic content was determined using the Folin-Ciocalteu spectrophotometric method (Nabavi et al., 2010). Briefly, 0.5 mL plant extract was mixed with 10% Folin-Ciocalteu reagent, followed by addition of 1 M Na_2CO_3 solution. After incubation in the dark at room temperature for 2 h, absorbance was measured at 760 nm. Gallic acid was used for calibration, and results were expressed as mg gallic acid equivalents (GAE) per g extract.

Total flavonoid content was determined spectrophotometrically using the aluminum chloride method (Chang et al., 2002). Briefly, plant extract was mixed with 20% $AlCl_3$ and potassium acetate solutions and incubated at room temperature for 30 min. Absorbance was measured at 415 nm. Quercetin was used for calibration, and results were expressed as mg quercetin equivalents (QE) per g extract.

Antioxidant activity

DPPH analysis. The 2,2-diphenyl-1-picrylhydrazyl (DPPH) radical scavenging activity was determined according to Molyneux (2004). Plant extract was mixed with DPPH solution (0.1 mM) and incubated at room temperature for 50 min in the dark. Absorbance was measured at 517 nm, and radical scavenging activity was calculated as percentage inhibition. The DPPH radical scavenging activity was calculated using the following equation:

$$\% \text{ DPPH} = (A_{control} - A_{sample})/A_{control} \times 100 \quad (1)$$

ABTS analysis. The 2,2'-azino-bis-3-ethyl-benzothiazoline-6-sulfonic acid (ABTS) radical scavenging activity was evaluated following the method of Re et al. (1999). The ABTS solution was prepared and diluted to an absorbance of 0.7 ± 0.05 at 734 nm. Plant extract was added to the ABTS solution and incubated for 6 min at room temperature. Absorbance was measured at 734 nm, and results were expressed as percentage inhibition. The ABTS radical scavenging activity was calculated using the following equation:

$$\% \text{ ABTS} = (A_{control} - A_{sample})/A_{control} \times 100 \quad (2)$$

FRAP analysis. The ferric reducing antioxidant power (FRAP) assay was performed according to Benzie and Strain (1996). Plant extract was incubated with FRAP reagent at 37 °C for 4 min, and absorbance was measured at 595 nm. Results were expressed as µmol Fe^{2+} equivalents per g extract.

AgNP synthesis and characterization

Plant extracts were mixed with 5 mM $AgNO_3$ solution at a ratio of 1:4 and incubated at 30 °C under dark conditions for 24 h with continuous shaking (150 rpm). The synthesized nanoparticles were collected by centrifugation at 5000 rpm for 15 min and stored at 4 °C.

The morphology and size of synthesized Ag nanoparticles (AgNPs) were analyzed using scanning electron microscopy (SEM). Elemental composition was determined by energy dispersive X-ray (EDX) spectroscopy. Functional groups involved in nanoparticle formation were identified using Fourier transform infrared (FTIR) spectroscopy (4000-400 cm^{-1}). Crystalline structure was analyzed by X-ray diffraction (XRD).

Antimicrobial activity

Antimicrobial activity of the synthesized AgNPs was tested against Gram-positive bacteria (*Enterococcus faecalis*, *Streptococcus pyogenes*, *Bacillus spizizenii*, *Bacillus subtilis*, *Staphylococcus aureus*), Gram-negative

bacteria (*Escherichia coli*, *Pseudomonas aeruginosa*, *Klebsiella pneumoniae*, *Klebsiella aerogenes*) and yeast (*Candida albicans*). Methanol was evaporated and extracts were dissolved in DMSO prior to testing. The disk diffusion method was used, and inhibition zones were measured using a digital caliper. Cefadroxil disks were used as positive control.

Minimum inhibitory concentration

The minimum inhibitory concentration (MIC) values of AgNPs derived from *H. perforatum* and *H. malatyanum* were determined using the broth macrodilution method. Two-fold serial dilutions of each nanoparticle suspension were prepared in Mueller-Hinton broth to obtain final concentrations ranging from 50 to 0.39 mg mL^{-1} (50, 25, 12.5, 6.25, 3.125, 1.56, 0.78, and 0.39 mg mL^{-1}). Each dilution was inoculated with 100 µL standardized microbial suspension (1.5×10^6 CFU mL^{-1}) and incubated at 37 °C for 24 h. Following incubation, the tubes were examined for turbidity, and the lowest concentration showing no visible microbial growth was recorded as the MIC value (Dhiman et al., 2021).

Statistical analyses

Data were analyzed using SPSS Statistics for Windows, Version 25.0 (IBM, Armonk, New York, USA). All experiments were performed in triplicate, and the results are presented as mean ± standard deviation (SD).

RESULTS AND DISCUSSION

A visible colour change from light brown to dark brown was observed immediately after the addition of the plant extracts to the $AgNO_3$ solution, indicating the reduction of Ag^+ ions and the formation of Ag nanoparticles (AgNPs). This colour transition, commonly observed during plant-mediated AgNP synthesis, is attributed to the surface plasmon resonance (SPR) phenomenon characteristic of metallic Ag nanoparticles and has been widely reported in previous studies (Ahmed et al., 2016).

Fourier transform infrared (FTIR) spectroscopy was employed to identify the functional groups involved in nanoparticle synthesis. The spectra recorded within the range of 4000-650 cm^{-1} exhibited characteristic absorption bands corresponding to hydroxyl, carbonyl, and amine groups (Figure 2). These functional groups are mainly associated with phenolic compounds, flavonoids, and proteins, which play essential roles in both the reduction of Ag^+ ions and the stabilization of the synthesized nanoparticles (Hemmati et al., 2019; Alahmad et al., 2022). These findings indicate that the rich phytochemical composition of *Hypericum* species acts not only as a reducing agent but also as a natural capping agent during nanoparticle biosynthesis.

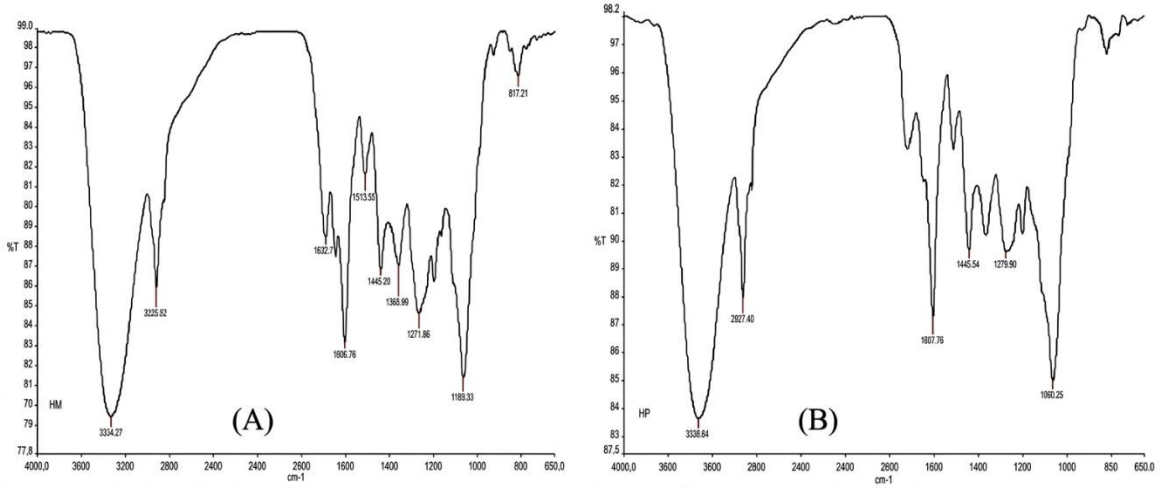

Figure 2. Fourier transform infrared (FTIR) spectra of Ag nanoparticles (AgNPs) synthesized using *Hypericum perforatum* (A) and *H. malatyanum* (B).

The X-ray diffraction (XRD) analysis revealed that the nanoparticles synthesized from both plant extracts lacked distinct diffraction peaks corresponding to crystalline metallic Ag and instead exhibited broad amorphous halos (Figure 3). This observation suggests that crystal growth may have been restricted by the adsorption of plant-derived biomolecules onto the nanoparticle surface. Such biomolecule-mediated stabilization has previously been reported to influence the surface characteristics and biological properties of biosynthesized nanoparticles (Ahmed et al., 2016).

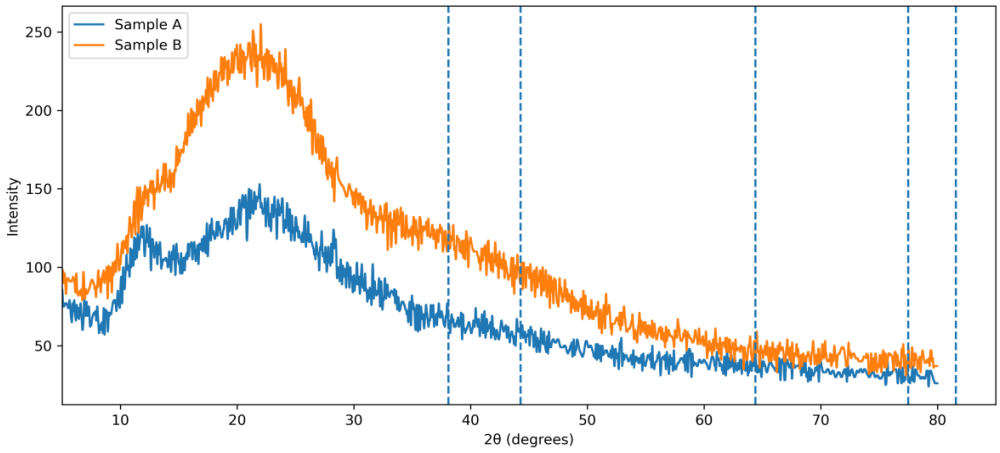

Figure 3. X-Ray diffraction (XRD) patterns of biosynthesized nanoparticles obtained from *Hypericum perforatum* (sample A) and *H. malatyanum* (sample B) with reference face-centered cubic Ag peak positions.

Energy-dispersive X-ray (EDX) analysis revealed the elemental composition of the synthesized nanoparticles. Characteristic signals corresponding to Ag, C, O, Cl, K, Ca, and Mg were detected in the spectra (Figures 4 and 5). While the presence of Ag confirmed the incorporation of Ag into the synthesized structures, the remaining elements were considered to originate from phytochemical constituents and mineral components of the plant extracts. These compounds are thought to remain adsorbed on the nanoparticle surface, contributing to nanoparticle stabilization. Similar elemental profiles have also been reported for nanoparticles synthesized using *Hypericum* extracts (Maleš et al., 2006).

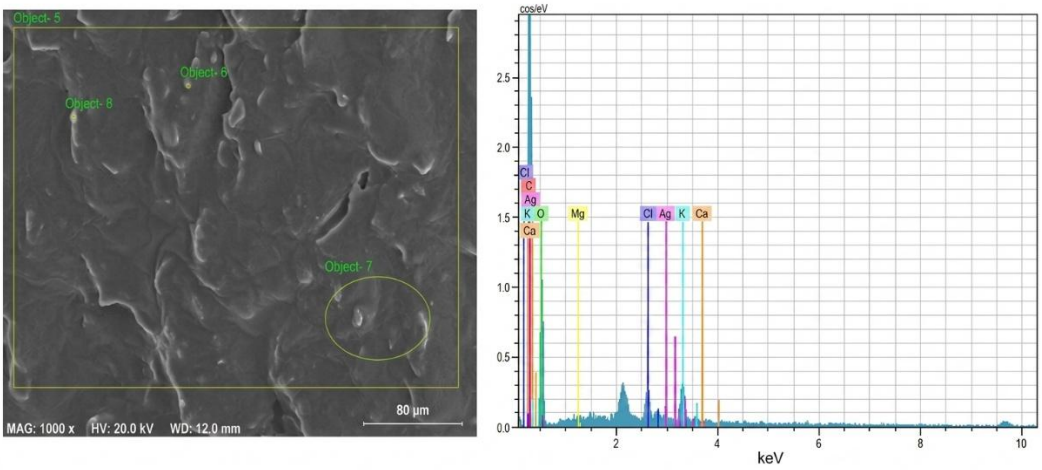

Figure 4. Energy dispersive X-ray (EDX) spectrum of *Hypericum perforatum* Ag nanoparticles (AgNPs).

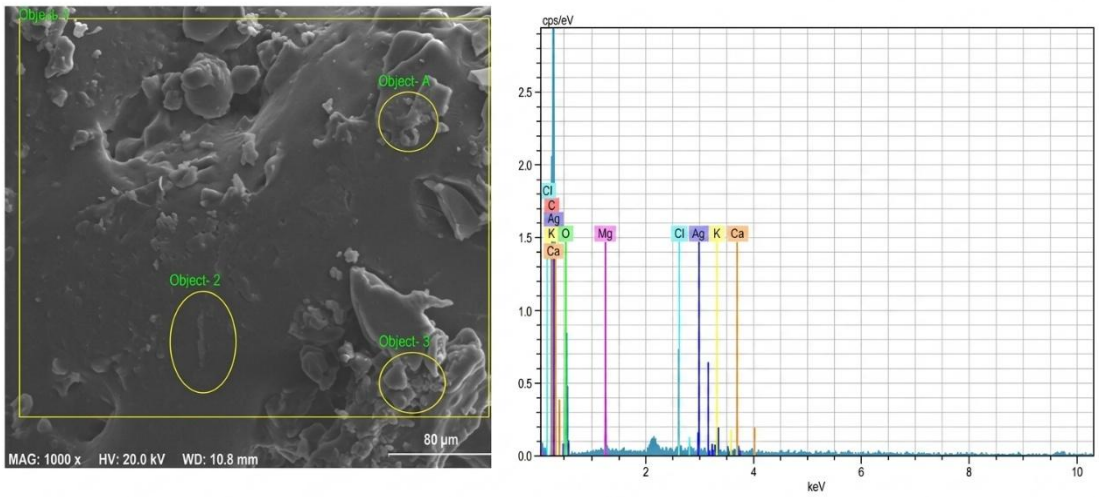

Figure 5. Energy dispersive X-ray (EDX) spectrum of *Hypericum malatyanum* Ag nanoparticles (AgNPs).

Scanning electron microscopy (SEM) analysis demonstrated that the synthesized nanoparticles were predominantly spherical and ranged in size from 1 to 80 nm (Figure 6). Nanoparticles within this size range possess a high surface-area-to-volume ratio, enabling more efficient interaction with microbial cells and consequently enhancing their biological activity. Similar particle sizes and morphologies have previously been reported for plant-mediated AgNPs synthesized using phenolic-rich plant extracts (Gitea et al., 2020).

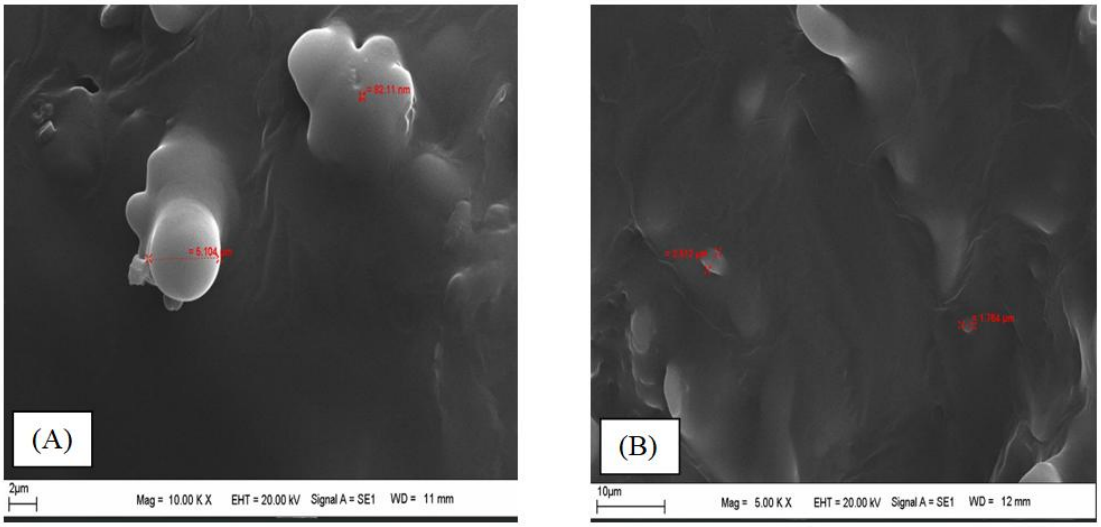

Figure 6. Scanning electron microscopy (SEM) analysis of Ag nanoparticles synthesized using *Hypericum perforatum* L. (A) and *H. malatyanum* Peşmen (B).

Phytochemical analysis demonstrated that both *Hypericum* species contained considerable amounts of phenolic and flavonoid compounds (Table 1). The endemic species *H. malatyanum* Peşmen exhibited a higher total phenolic content (231.4 ± 5.8 mg gallic acid equivalents [GAE] g^{-1}) than *H. perforatum* L. (216.9 ± 4.4 mg GAE g^{-1}). Similarly, DPPH radical scavenging activity was higher in *H. malatyanum* (79.9 ± 0.9%) than in *H. perforatum* (73.8 ± 1.6%). The FRAP assay also demonstrated a greater reducing capacity for *H. malatyanum* (315.5 ± 8.6 µmol Fe^{2+} g^{-1}) compared with *H. perforatum* (269.6 ± 7.7 µmol Fe^{2+} g^{-1}). In contrast, *H. perforatum* exhibited higher total flavonoid content (31.3 ± 2.5 mg QE g^{-1}) and ABTS radical scavenging activity (57.4 ± 1.9%) than *H. malatyanum*.

Table 1. Phytochemical content and antioxidant activities of *Hypericum* extracts as mean ± SD (n = 3). GAE: Gallic acid equivalents; QE: quercetin equivalents; DPPH: 2,2-diphenyl-1-picrylhydrazyl; ABTS: 2,2'-azino-bis-3-ethyl-benzothiazoline-6-sulfonic acid; FRAP: ferric reducing antioxidant power.

	Total phenolic content	Total flavonoid content	DPPH	ABTS	FRAP
	mg GAE g^{-1}	mg QE g^{-1}	%	%	µmol Fe^{2+} g^{-1}
H. perforatum	216.9 ± 4.4	31.3 ± 2.5	73.8 ± 1.6	57.4 ± 1.9	269.6 ± 7.7
H. malatyanum	231.4 ± 5.8	18.6 ± 1.0	79.9 ± 0.9	45.8 ± 0.6	315.5 ± 8.6

The strong reducing capacity of phenolic compounds facilitates the conversion of Ag^+ ions into metallic Ag while simultaneously preventing nanoparticle aggregation through surface capping. In particular, hydroxyl groups donate electrons during the reduction process, thereby promoting nanoparticle formation and contributing to the production of more stable and biologically active nanoparticles (Srikar et al., 2016). Therefore, the higher total phenolic content and antioxidant capacity observed in *H. malatyanum* are likely responsible for the enhanced biological activity of the corresponding AgNPs.

The antimicrobial activity results (Table 2) demonstrated that AgNPs synthesized from both plant extracts produced larger inhibition zones than their corresponding crude extracts. The highest antimicrobial activity was observed for *H. malatyanum*-derived AgNPs against *Bacillus spizizenii*, with an inhibition zone of 7.45 ± 0.09 mm, whereas the corresponding inhibition zone produced by *H. perforatum*-derived AgNPs was 4.75 ± 0.07 mm. Similarly, *H. malatyanum*-derived AgNPs exhibited greater antimicrobial activity against *Escherichia coli*, *Streptococcus pyogenes*, *Klebsiella pneumoniae*, and *Candida albicans* than those synthesized using *H. perforatum*.

Table 2. Antimicrobial activities of crude extracts and biosynthesized AgNPs derived from *Hypericum perforatum* and *H. malatyanum* against selected microorganisms. All assays were performed in triplicate, and the results are presented as mean ± SD. AgNPs: Ag nanoparticles; NA: no activity.

	Zone diameter (mm)				
	Hypericum perforatum	*Hypericum malatyanum*	AgNP *H. perforatum*	AgNP *H. malatyanum*	Cefadroxil
Enterococcus faecalis	2.3 ± 0.02	2.5 ± 0.012	3.62 ± 0.025	4.24 ± 0.052	10.0 ± 0.96
Escherichia coli	1.5 ± 0.002	NA	4.9 ± 0.051	6.05 ± 0.045	9.5 ± 0.78
Streptococcus pyogenes	3.2 ± 0.004	2.5 ± 0.012	4.86 ± 0.060	3.65 ± 0.021	9.3 ± 0.83
Pseudomonas aeruginosa	NA	NA	1.76 ± 0.011	3.34 ± 0.031	10.5 ± 1.08
Bacillus spizizenii	2.4 ± 0.03	3.1 ± 0.022	3.23 ± 0.042	7.45 ± 0.087	10.7 ± 1.86
B. subtilis	2.3 ± 0.021	2.5 ± 0.031	3.36 ± 0.044	4.25 ± 0.041	8.5 ± 0.93
Klebsiella pneumoniae	3.1 ± 0.032	4.12 ± 0.05	4.34 ± 0.050	6.15 ± 0.071	11.3 ± 1.56
Staphylococcus aureus	2.3 ± 0.04	NA	4.54 ± 0.056	5.33 ± 0.051	12.2 ± 1.87
K. aerogenes	NA	1.5 ± 0.041	1.7 ± 0.021	4.65 ± 0.044	9.54 ± 1.01
Candida albicans	NA	NA	1.0 ± 0.09	NA	NA

The superior antimicrobial activity of AgNPs compared with crude extracts can be attributed not only to the antimicrobial properties of Ag but also to the synergistic interaction between AgNPs and plant-derived phytochemicals. Ag nanoparticles attach to the microbial cell wall, disrupt membrane integrity, increase membrane permeability, stimulate the production of reactive oxygen species (ROS), and inhibit essential enzymes and DNA replication through the sustained release of Ag^+ ions, ultimately leading to microbial cell death. Furthermore, naturally occurring phytochemicals in *Hypericum* species, including hypericin, hyperforin, and flavonoids, may further contribute to antimicrobial activity, thereby enhancing the efficacy of biosynthesized AgNPs (Patra and Baek, 2016).

The minimum inhibitory concentration (MIC) results further supported the disk diffusion findings (Figure 7). The MIC values of *H. perforatum*-derived AgNPs ranged from 12.5 to 25 mg mL^{-1}, whereas those of *H. malatyanum*-derived AgNPs ranged from 6.25 to 12.5 mg mL^{-1}. The lowest MIC value (6.25 mg mL^{-1}) was

recorded against *Bacillus spizizenii*, *Streptococcus pyogenes*, *Enterococcus faecalis*, and *Klebsiella pneumoniae*. In contrast, the corresponding MIC value for *H. perforatum*-derived AgNPs against these microorganisms was 12.5 mg mL^{-1}. Lower MIC values indicate that microbial growth can be inhibited with lower nanoparticle concentrations, confirming the superior antimicrobial efficacy of *H. malatyanum*-derived AgNPs.

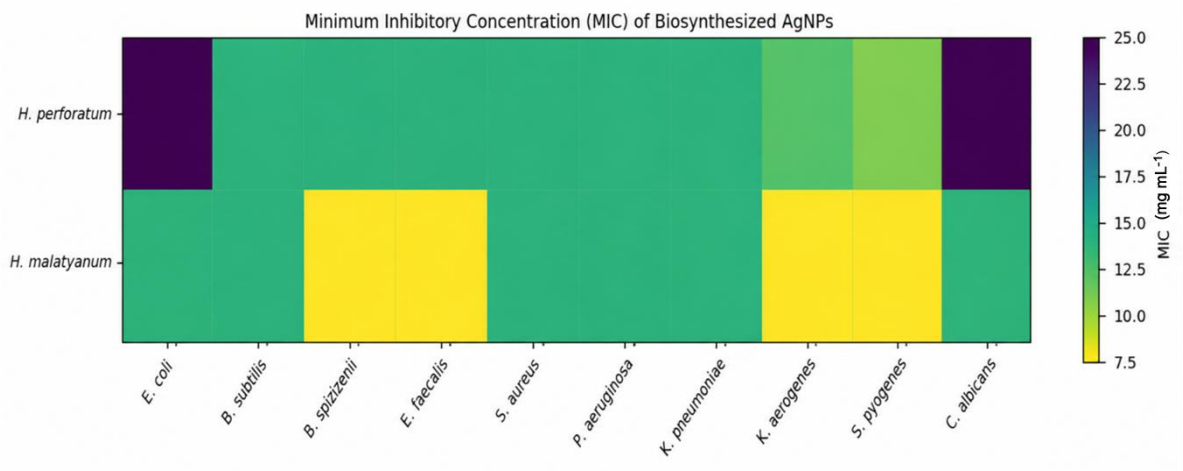

Figure 7. Heatmap showing the minimum inhibitory concentration (MIC) values of biosynthesized AgNPs derived from *Hypericum perforatum* and *H. malatyanum* against selected microorganisms. Lower MIC values and lighter colors indicate stronger antimicrobial activity. *Escherichia coli*, Bacillus subtilis, *B. spizizenii*, *Enterococcus faecalis*, *Staphylococcus aureus*, *Pseudomonas aeruginosa*, *Klebsiella pneumoniae, K. aerogenes, Streptococcus pyogenes*, *Candida albicans*.

The lower MIC values exhibited by *H. malatyanum*-derived AgNPs may be attributed to the higher phenolic content and antioxidant capacity of this species, which promote more efficient reduction and stabilization during nanoparticle synthesis. Smaller nanoparticles with greater surface reactivity interact more effectively with microbial cell surfaces, release higher amounts of Ag^{+} ions, and induce stronger oxidative stress, thereby inhibiting microbial growth at lower concentrations. Similar findings have been reported for AgNPs synthesized using extracts of *Hypericum hookerianum*, *H. scabrum*, *Origanum vulgare*, and *Carduus crispus* (Manoj et al., 2015; Urnukhsaikhan et al., 2021).

Overall, the present study demonstrated that extracts of *H. perforatum* and the endemic species *H. malatyanum* are effective biological resources for the green synthesis of biologically active AgNPs. The higher phenolic content and antioxidant capacity of *H. malatyanum* were associated with stronger antimicrobial activity and lower MIC values of the synthesized AgNPs. These findings demonstrate that phytochemical composition plays a decisive role in nanoparticle formation and biological performance, highlighting the potential of endemic plant species as sustainable and eco-friendly bioresources for the development of antimicrobial nanomaterials with prospective applications in agriculture, food preservation, and biomedicine.

CONCLUSIONS

The results of this study demonstrate that both *Hypericum perforatum* and the endemic *H. malatyanum* possess significant phytochemical potential for the green synthesis of Ag nanoparticles (AgNPs). The obtained Ag-containing nanoscale structures exhibited predominantly spherical morphology with sizes ranging from 1 to 80 nm. Fourier transform infrared spectroscopy and energy dispersive X-ray spectroscopy analyses indicated the involvement of plant-derived biomolecules and the presence of Ag, whereas X-ray diffraction patterns revealed limited crystallinity and a predominantly amorphous structure.

Comparative evaluation revealed that nanoparticles synthesized using *H. malatyanum* showed stronger antimicrobial activity and lower minimum inhibitory concentration values against several tested microorganisms

than those synthesized from *H. perforatum*. These findings indicate that differences in phytochemical composition, particularly phenolic and flavonoid content, play a decisive role in nanoparticle synthesis efficiency and biological performance.

The enhanced antimicrobial activity observed in plant-mediated AgNPs suggests their potential application as eco-friendly antimicrobial agents. In particular, these results highlight the possible use of such nanoparticles in agricultural systems for plant disease management and post-harvest protection.

Overall, this study confirms that endemic plant species can serve as effective bioresources for the development of sustainable nanomaterials with potential applications in agriculture and related fields.

Author contribution

E.Ö. designed the study and wrote the manuscript.

Acknowledgements

The author would like to thank Prof. Dr. Şanlı Kabaktepe (Malatya Turgut Özal University) and Asst. Prof. Dr. Şükrü Karakuş (İnönü University) for their support in providing the plant materials used in this study.

References

Ahmed, S., Saifullah, Ahmad, M., Swami, B.L., Ikram, S. 2016. Green synthesis of silver nanoparticles using plant extracts and their antimicrobial activities: A review. Journal of Advanced Research 7:17-28.

Alahmad, A., Alghoraibi, I., Zein, R., Kraft, S., Dräger, G., Walter, J., et al. 2022. Identification of major constituents of *Hypericum perforatum* L. extracts by HPLC-ESI-Q-TOF MS and their antioxidant activities. ACS Omega 7:13475-13493.

Alowaiesh, B.F., Awad, N.S., Eldenary, M.E., El Moneim, D.A. 2024. Farklı biyostimülan nanopartiküller kullanılarak patateste kuraklık toleransının artırılması. Şili Tarım Araştırmaları Dergisi 84:246-259. doi:10.4067/S0718-58392024000200246.

Baran, M.F. 2019. Synthesis, characterization and antimicrobial activity of silver nanoparticles from *Cydonia oblonga* leaf. Applied Ecology and Environmental Research 17:2583-2592.

Benzie, I.F., Strain, J.J. 1996. The ferric reducing ability of plasma (FRAP) as a measure of antioxidant power. Analytical Biochemistry 239:70-76.

Chang, C.C., Yang, M.H., Wen, H.M., Chern, J.C. 2002. Estimation of total flavonoid content by colorimetric methods. Journal of Food and Drug Analysis 10:178-182.

Crockett, S.L., Robson, N.K.B. 2011. Taxonomy and chemotaxonomy of the genus *Hypericum*. Medicinal and Aromatic Plant Science and Biotechnology 5:1-13.

Çiftçi, Y.Ö., Altınkut-Uncuoğlu, A. 2019. Current approaches in plant biotechnology. Palme Publishing, Ankara, Türkiye.

Çırak, C., Kurt, D. 2014. *Hypericum* species as medicinal plants. Anatolia Journal of AARI 24:42-58.

Dhiman, R., Aggarwal, N.K., Aneja, K.R., Kaur, M. 2021. In vitro antimicrobial activity and phytochemical studies of *Terminalia chebula* against microbes isolated from fruit juices. Journal of Microbiology, Biotechnology and Food Sciences 2021:243-247.

Dirmenci, T., Robson, N.K.B. 2019. Two new taxa of *Hypericum* from Turkey. Kew Bulletin 74:66.

Gitea, D., Teodorescu, A.G., Pantis, C., Tit, D.M., Bungau, A.F., Bogdan, M., et al. 2020. Green synthesis of silver nanoparticles using *Hypericum perforatum* L. extract and evaluation of their antibacterial activity. Revista de Chimie 71:273-279.

Güner, A., Aslan, S., Ekim, T., Vural, M., Babaç, M.T. (eds.) 2012. List of plants in Turkey (vascular plants). Nezahat Gökyiğit Botanik Bahçesi Yayınları, İstanbul, Türkiye.

Hemmati, S., Rashtiani, A., Zangeneh, M.M., Zangeneh, A., Veisi, H. 2019. Green synthesis of silver nanoparticles using *Fritillaria* extract and evaluation of their biological activities. Polyhedron 158:8-14.

Maleš, Ž.A., Kremer, D., Žuntar, I., Babić, S. 2006. Phytochemical investigations of *Hypericum perforatum* L. Acta Pharmaceutica 56:359-367.

Manoj, L., Vishwakarma, V., Samal, S.S., Seeni, S. 2015. Green synthesis of silver nanoparticles using hypericin-rich shoot cultures of *Hypericum hookerianum* and evaluation of antibacterial activity. Journal of Experimental Nanoscience 10:181-188.

Molyneux, P. 2004. The use of DPPH for estimating antioxidant activity. Songklanakarin Journal of Science and Technology 26:211-219.

Nabavi, S.F., Ebrahimzadeh, M.A., Nabavi, S.M., Hamidinia, A., Bekhradnia, A.R. 2010. Antioxidant activity of *Vitis vinifera* L. leaf extracts. Grasas y Aceites 61:244-250.

Ojo, O.A., Ojo, A.B., Akinwumi, O.J., Ajiboye, B.O., Oyinloye, B.E. 2017. Green synthesis of silver nanoparticles using plant extracts and their biological activities. Journal of Bionanoscience 11:292-296.

Özbey, E., Asma, D., Kabaktepe, Ş. 2025. Comparison of antimicrobial, antioxidant activities and chemical contents of endemic *Hypericum malatyanum* and *Hypericum perforatum* species growing in Malatya. Pakistan Journal of Botany 57(5). doi:10.30848/PJB2025-5(30).

Patil, M.P., Kim, G.D. 2018. Antibacterial potential of silver nanoparticles synthesized using *Lactobacillus plantarum* culture supernatant. Microbial Pathogenesis 121:184-189.

Patra, J.K., Baek, K.H. 2016. Green nanobiotechnology: Factors affecting synthesis and characterization techniques of phyto-mediated biosynthesized silver nanoparticles. Journal of Photochemistry and Photobiology B: Biology 161:200-210.
Peşmen, H. 1980. Six new species from Anatolia. Notes from the Royal Botanic Garden Edinburgh 38:435-441.
Popay, I. 2015. *Hypericum perforatum* (St John's wort). In CABI Invasive Species Compendium. CAB International, Wallingford, UK.
Re, R., Pellegrini, N., Proteggente, A., Pannala, A., Yang, M., Rice-Evans, C. 1999. Antioxidant activity applying an improved ABTS radical cation decolorization assay. Free Radical Biology and Medicine 26:1231-1237.
Saravanakumar, K., Chelliah, R., MubarakAli, D., Oh, D.H., Kathiresan, K., Wang, M.H. 2018. Green synthesis and characterization of biologically active nanosilver using marine algae and evaluation of antimicrobial activity. Journal of Photochemistry and Photobiology B: Biology 185:126-135.
Satpathy, S., Patra, A., Ahirwar, B., Hussain, M.D. 2018. Antioxidant and anticancer activities of green synthesized silver nanoparticles using plant extracts. Artificial Cells, Nanomedicine and Biotechnology 46:S71-S85.
Srikar, S.K., Giri, D.D., Pal, D.B., Mishra, P.K., Upadhyay, S.N. 2016. Green synthesis of silver nanoparticles: A review. Green and Sustainable Chemistry 6:34-56.
Urnukhsaikhan, E., Bold, B.E., Gunbileg, A., Sukhbaatar, N., Mishig-Ochir, T., Park, J.H. 2021. Antibacterial activity of silver nanoparticles biosynthesized using *Carduus crispus* extract. Scientific Reports 11:21047.